Soluble epoxide hydrolase deficiency alters pancreatic islet size and improves glucose homeostasis in a model of insulin resistance

Ayala Luria[a,1], Ahmed Bettaieb[b,1], Yannan Xi[b], Guang-Jong Shieh[a], Hsin-Chen Liu[a], Hiromi Inoue[c], Hsing-Ju Tsai[a], John D. Imig[d], Fawaz G. Haj[b,2], and Bruce D. Hammock[a,e,2]

[a]Departments of Entomology; and [b]Nutrition; [c]Department of Internal Medicine, Division of Nephrology, School of Medicine; and the [e]Cancer Center, University of California, Davis, CA 95616; and [d]Department of Pharmacology and Toxicology, Cardiovascular Research Center, Medical College of Wisconsin, Milwaukee, WI 53226

Contributed by Bruce D. Hammock, March 14, 2011 (sent for review September 8, 2010)

Visceral obesity has been defined as an important element of the metabolic syndrome and contributes to the development of insulin resistance and cardiovascular disease. Increasing endogenous levels of epoxyeicosatrienoic acids (EETs) are known for their analgesic, antihypertensive, and antiinflammatory effects. The availability of EETs is limited primarily by the soluble epoxide hydrolase (sEH, *EPHX2*), which metabolizes EETs to their less active diols. In this study, we tested the hypothesis that EETs are involved in glucose regulation and in retarding the development of insulin resistance. To address the role of EETs in regulating glucose homeostasis and insulin signaling, we used mice with targeted gene deletion of sEH (*Ephx2*-null mice) and a subsequent study with a selective sEH inhibitor. When wild-type mice are fed a high fat diet, insulin resistance develops. However, knockout or inhibition of sEH activity resulted in a significant decrease in plasma glucose. These findings are characterized by enhancement of tyrosyl phosphorylation of the insulin receptor, insulin receptor substrate 1, and their downstream cascade. In addition, pancreatic islets were larger when sEH was disrupted. This effect was associated with an increase in vasculature. These observations were supported by pharmacological inhibition of sEH. These data suggest that an increase in EETs due to sEH-gene knockout leads to an increase in the size of islets and improved insulin signaling and sensitivity.

type 2 diabetes | pancreas | arachidonic acid pathway

Obesity is an increasingly important public health issue (1). Obese individuals exhibit a higher risk of chronic diseases including cardiovascular disease and type 2 diabetes. The latter is a complex, polygenic disease wherein a number of tissues are rendered insulin resistant (2). Insulin action is mediated by a complex network of signaling events that modulate glucose homeostasis (3). A fundamental mechanism for the maintenance of glucose homeostasis is the rapid action of insulin to stimulate glucose uptake and metabolism in peripheral tissues. This cascade is initiated by binding of insulin to its cell surface receptor, followed by receptor autophosphorylation, which results in tyrosine phosphorylation of insulin receptor substrates (IRSs) and downstream signaling molecules (4, 5). The mechanism underlying insulin resistance in type 2 diabetes contains many signaling players (6, 7), and results from pancreatic β-cell insufficiency with impairment of glucose-stimulated insulin secretion (8) and impaired insulin receptor signaling (9).

Epoxyeicosanoids or EETs are thought to be one of multiple classes of chemical mediators which influence insulin production and sensitivity. EET regioisomers (5,6-, 8,9-, 11,12-, and 14,15-EET) are formed from arachidonic acid by epoxidation by cytochrome P450 monoxygenases (10). EETs mediate endothelium-dependent vasodilation, promote angiogenesis, are antiinflammatory, and have analgesic properties (11–13). The soluble epoxide hydrolase (sEH) adds water to epoxides forming 1,2-diols. In the case of EETs it forms dihydroxy eicosanoids or DHETs (14). For most biological endpoints so far investigated, EETs are more biologically active than the corresponding DHETs. Also DHETs are rapidly conjugated and excreted (15). Polymorphism of the sEH gene is associated with insulin resistance (16). Thus mice deleted of the sEH gene or treated with inhibitors of the sEH (sEHI) are valuable probes for testing if EETs are involved in insulin sensitivity and glucose regulation.

In addition to their salutary effects in the vasculature, EETs might have beneficial effects on lipid metabolism and insulin sensitivity. For example, sEH protein and message levels are up regulated in the epididymal fat pad from mice that received a high fat diet (HFD) (17). In addition, cytochrome P450 2C (CYP2C) expression is decreased and sEH expression is increased in obese Zucker rats, a commonly used animal model of obesity and insulin resistance (18). In a type 1 diabetes model, genetic and pharmacological inhibition of sEH results in increased insulin secretion and attenuation of hyperglycemia (18). sEH inhibition is a well established approach in cardiovascular, renal, and inflammatory diseases in murine models, but its contribution in type 2 diabetes mellitus remains to be established. This study was designed to investigate the roles of EETs in insulin resistance and glucose regulation by modulating the activity of sEH with genetic and pharmacological tools.

Results

Whole-Body Soluble Epoxide Hydrolase Deletion and Inhibition in Mice. To investigate the role of sEH in regulating glucose homeostasis, we assessed the physiological effects of its removal. Disruption of sEH was achieved through the use of whole-body knockout (KO, *Ephx2*-null) mice (19, 20) and pharmacological inhibition using a selective sEH inhibitor (21). A PCR product of 290 bp indicates the *Ephx2* sequence that distinguished wild type (WT) from KO mice (band of 560 bp represents the sequence of neomycin gene) (Fig. 1*A*). Immunoblot analysis was used to determine the efficiency of sEH deletion in different tissues including those that are insulin-responsive (Fig. 1*B*). sEH protein was expressed in all examined tissue extracts of WT mice, and was absent in KO mice indicating efficient deletion of the gene

Author contributions: A.L., A.B., J.D.I., F.G.H., and B.D.H. designed research; A.L. and A.B. performed research; H-C.L., G-J.S., and H-J.T helped with animal experiments; Y.X., and H.I. performed histochemistry experiments; A.L. and A.B. analyzed data; and A.L., A.B., J.D.I, F.G.H., and B.D.H. wrote the paper.

Conflict of interest statement: Several of the authors are authors of intellectual property in the areas of treating metabolic disease, inflammation, pain, hypertension, and other disorders by the manipulation of oxylipins, and the use of inhibitors of the soluble epoxide hydrolase (A.L., A.B., F.G.H., H-J.T., J.D.I., and B.D.H.).

[1]A.L. and A.B. contributed equally to this work.

[2]To whom correspondence may be addressed. E-mail: bdhammock@ucdavis.edu or fghaj@ucdavis.edu.

This article contains supporting information online at www.pnas.org/lookup/suppl/doi:10.1073/pnas.1103482108/-/DCSupplemental.

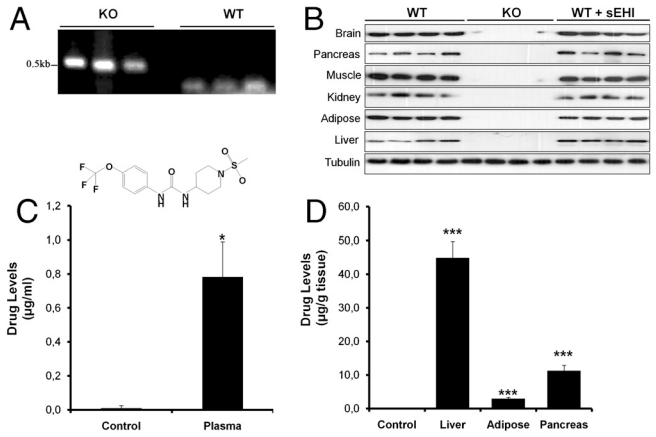

Fig. 1. Whole-body Ephx2 gene deletion and sEH inhibition. (*A*) Representative genotype analysis using genomic DNA from murine tails. PCR product of sEH sequence recognizes a 290-bp gene product in WT animals, while a gene product of the neomycin resistant gene (560-bp) is shown in KO null mice. (*B*) Immunoblots of sEH in different tissues from WT, KO mice, and sEHI-treated WT mice that were taken at the end of the study (6 mo). Tubulin expression is shown as a control for loading. (*C*) Plasma and (*D*) tissue concentrations of TUPS (structure shown) from WT mice that are untreated (control) and treated with TUPS ($n = 4$) for 6 mo. Values depict mean ± SEM of $n = 4$. * $P \leq 0.05$, and *** $P \leq 0.001$ *t*-test of WT untreated vs. WT treated with TUPS.

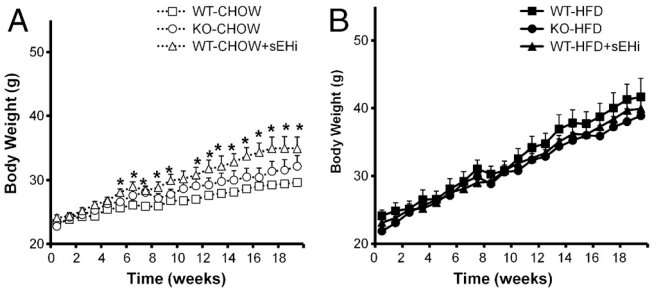

Fig. 2. Body weights of KO, sEHI-treated and WT mice fed chow or high fat diet. Body weight of age-matched wild type (WT), KO, and WT mice treated with a TUPS, 10 mg/L via drinking water fed regular chow diet (CHOW) (*A*) or a HFD (*B*) for 20 weeks post weaning. Values depict mean ± SEM of $n = 4$. *t*-test, * $P \leq 0.05$, WT-chow vs. WT-chow + sEHI.

(Fig. 1*B*). As expected, treatment of WT mice with a sEHI did not alter sEH expression (Fig. 1*B*).

sEH contains both the epoxide hydrolase and phosphatase domains. To ensure that effects are attributed to the epoxide hydrolase domain, we used a selective epoxide hydrolase inhibitor. Pharmacological inhibition was achieved by treating animals with selective sEH inhibitor (TUPS). This compound is an effective inhibitor of sEH (IC_{50} of 5 and 3 nM for murine and human sEH, respectively) (22, 23). The concentration of TUPS in blood and tissue extracts was determined at the end of the study. TUPS concentrations in blood ranged between 800–1,000 ng/mL (2–3 μM TUPS) (Fig. 1*C*). These levels are significantly higher than the IC_{50} concentration determined with in vitro experiments using the recombinant murine sEH enzyme (21, 24). Additionally, liver, epididymal fat, and pancreas extracts revealed elevated levels of TUPS, with liver homogenates exhibiting the highest concentrations (45 μg/g tissue or 0.12 μmol/g tissue) compared with epididymal fat and pancreas [3 and 10 μg/g tissues, or 0.01 and 0.026 μmol/g tissue, respectively (Fig. 1*D*)]. These blood and tissue levels of sEHI increase epoxy-fatty acid to diol ratios in both plasma and tissue (22). Taken together, these findings indicate that KO mice exhibit efficient gene deletion and indicate that the sEH inhibitor is distributed to tissues.

Effects of sEH Gene Deletion and Inhibition on Body Mass and Adiposity. To study the role of sEH in body mass regulation, WT, KO, and sEHI-treated WT mice were fed regular chow or HFD, and body weights and food intake were measured weekly. As expected, mice on a HFD gained significantly more weight than their counterparts on chow diet but no differences were observed among genotypes on HFD (Fig. 2). However, mice treated with sEHI gained significantly more weight than their counterparts on chow diet (Fig. 2*A*, Fig. S1). Consistent with the increased body weight in mice on HFD, adiposity was comparably increased (Fig. S2). In addition, H and E staining of tissues from mice on chow and HFD did not reveal any pathological effects of sEH deletion or inhibition (Fig. S3).

Improved Insulin Sensitivity and Glucose Tolerance Mice with *Ephx2* Deletion and sEH Inhibition. Several metabolic parameters were assayed in KO, WT, and sEHI-treated WT mice on chow and a HFD (Table 1). These parameters were analyzed in both fasted and fed conditions. Despite their similar body weights and adiposity, fasted glucose levels in KO mice on a HFD were lower than those of WT and sEHI-treated mice (Table 1). When animals were fed, glucose levels on HFD were lower only when sEH was inhibited with TUPS, while on chow diet, glucose levels were comparable (Table 1). Consistent with this observation, sEHI-treated and KO mice exhibited lower levels of serum insulin levels on HFD compared with WT mice (Table 1). On chow diet, only KO mice showed lower levels of serum insulin (Table 1 fed conditions). When the ratio of insulin to glucose was calculated, KO mice either on chow or a HFD exhibited lower insulin to glucose ratios compared with WT counterparts, suggesting improved insulin sensitivity. sEHI-treated WT mice exhibited lower glucose levels, serum insulin levels, and insulin to glucose ratios only when they were not fasting and on HFD (Table 1). It is suggested that the increased weight in this group (Fig. 1*A*) masks differences in these parameters. In addition, several other parameters of whole-body homeostasis were measured. As expected, mice on HFD exhibited higher plasma leptin levels compared with those on chow diet. In line with their increased body weight on chow, sEHI-treated mice exhibited significantly higher levels of leptin compared with WT mice (Table 1). Leptin is critically involved in the regulation of body energy balance via its central actions on food intake and energy expenditure, and the effect of eicosanoids on leptin warrants further investigation. No significant alterations in adiponectin, an insulin-sensitizing adipokine (25) were observed. Finally, no significant differences were seen in triglyceride levels in mice fed HFD. However, when mice were on chow diet, inhibition of sEH tends to increase serum levels of triglycerides (Table 1, fed conditions).

To directly assess glucose responsiveness to insulin, mice were further subjected to insulin tolerance tests (ITTs) at two (Fig. S4 *A* and *B*) and 5 mo (Fig. 3 *A* and *B*) of age. While no differences in glucose levels following insulin injection were observed when mice were fed chow diet (Fig. 3*A*), significant differences were observed when sEH was disrupted on HFD at 2 and 5 mo. (Fig. S4*B*, Fig. 3*B*). On HFD, basal glucose levels were lower in KO and sEHI-treated mice compared with WT mice (Fig. 3*B*). Following insulin injection, KO and sEHI-treated WT mice exhibited significantly greater reduction in blood glucose compared with WT mice (Fig. 3*B*). Glucose levels were lower and significantly different in KO and sEHI-treated WT mice during the first 30 min, compared with WT-HFD mice (Fig. 3*B*). During the following 45–120 min, glucose levels tended to be lower in KO and sEHI-treated mice compared with WT but did not reach statistical significance (Fig. 3*B*). These findings were reproduced in another independent cohort of WT and KO mice on chow or HFD for three months (Fig. S4*E*). In addition to their improved responsiveness to insulin, KO and sEHI-treated mice exhibited improved ability to clear glucose from the peripheral

Table 1. Metabolic parameters of WT, sEHI-treated and KO mice

	CHOW			HFD		
	WT	KO	WT + sEHI	WT	KO	WT + sEHI
Glucose (mg/dL)						
Fed	194 ± 2.6*	180 ± 8.8*	184 ± 9.3	218 ± 7.7†	224 ± 8.5§	170 ± 14.1†§
Fasted	115 ± 12.5*	101 ± 5.3*	138 ± 21	168±4.5‡	137 ± 9.2	167±3.1§
Serum insulin (mg/mL)						
Fed	0.69 ± 0.1*	0.5 ± 0.1*	1.2 ± 0.28§	4.5 ± 1.6	2.8 ± 0.7	1.7 ± 0.6
Fasted	0.54 ± 0.2	0.46 ± 0.1	1.2 ± 0.4	0.8 ± 0.1	0.75 ± 0.2	0.7 ± 0.02
Insulin/glucose ratio						
Fed	0.35 ± 0.04*	0.31 ± 0.04*§	0.67 ± 0.1†, §	2.2 ± 0.8†	1.25 ± 0.4	0.96 ± 0.3
Fasted	0.45 ± 0.1	0.46 ± 0.01	0.89 ± 0.3	0.5 ± 0.06	0.55 ± 0.1	0.43 ± 0.01
Leptin (ng/mL)						
Fed	8.8 ± 0.4*	13.3 ± 2.6	16.5 ± 1.7†	21.7 ± 1.8	21.3 ± 2.9	20.6 ± 1.3
Fasted	3.2 ± 0.3*	3.9 ± 1.1*	12.7 ± 0.6†*	18.2 ± 1.6	19.5 ± 2.1	19.7 ± 1.6
Adiponectin (μg/mL)						
Fed	6.3 ± 0.8	5.0 ± 0.4	5.8 ± 0.8	5.6 ± 0.35	5.3 ± 0.6	5.5 ± 0.06
Fasted	6.7 ± 0.4	6.6 ± 0.1*	7.0 ± 0.8	4.6 ± 1.3	4.8 ± 0.1	4.3 ± 1.9
Triglycerides (mg/mL)						
Fed	0.48 ± 0.1	0.8 ± 0.06‡*	0.64 ± 0.03*	0.4 ± 0.04	0.4 ± 0.05	0.3 ± 0.04
Fasted	0.29 ± 0.01	0.3 ± 0.04*	0.27 ± 0.03*	0.4 ± 0.03	0.43 ± 0.02	0.4 ± 0.02

Serum was collected from fed and fasted (over night) male WT, KO, and WT + sEHI mice (five months on chow or HFD), and the indicated metabolic parameters were measured. Values are expressed as the mean ± SEM of measurements obtained from four animals per genotype.
Significant difference ($P < 0.05$) between HFD and Chow.
†significant difference between WT and WT + sEHI.
‡indicates significant difference between KO and WT mice.
§significant difference between KO and WT + sEHI-treated group.

circulation during an intraperitoneal (i.p.) glucose tolerance test when fed HFD for 2 mo (Fig. S4*D*). In contrast to ITT where mice were fasted for only 4 h, in glucose tolerance test (GTT) mice were fasted over night, hence the lower basal glucose levels (Fig. 3 *C* and *D*, Fig. S4 *C* and *D*). In this case, glucose was injected and the clearance rate was measured over 120 min. Faster glucose clearance from blood was observed in KO and sEHI-treated mice compared with WT mice fed HFD for 2 mo (Fig. S4*D*). Calculated area under the curve in KO and sEHI-treated mice was significantly lower than WT mice ($44{,}300 \pm 1{,}100$ mg/dL ∗ min, $45{,}300 \pm 2{,}100$, and $54{,}400 \pm 3{,}900$ mg/dL ∗ min, respectively) (Fig. S4*D*). Supporting data from another cohort study with WT and KO mice are shown in Fig. S4*F*. Over 5 mo of treatment, sEHI-treated mice failed to show improved glucose tolerance on HFD (Fig. 3*D*), while KO mice exhibited enhanced glucose tolerance on both chow and HFDs (Fig. 3 *C* and *D*). As shown in Fig. 3*C*, plasma glucose clearance is faster in KO mice on chow diet compared with WT and sEHI-treated mice.

To test whether the difference observed in GTT was caused by alterations in insulin levels, serum insulin concentrations were measured at 0, 15, and 30 min during GTTs. Plasma glucose levels were lower in KO and sEHI-treated mice on chow compared with WT mice, and on HFD only KO mice exhibited lower glucose levels (Table 2). After glucose administration, KO mice on chow and HFD exhibited a trend for increased insulin concentrations at 15 min, although that did not reach statistical significance. By 30 min, KO mice on chow exhibited higher insulin concentrations compared with WT mice (Table 2). Taken together, our findings demonstrate that sEH deficiency or inhibition directly improves systemic glucose homeostasis.

Effect of sEH Deletion and Inhibition on Pancreatic Islet Size and Vascularization. To better understand the mechanism underlying enhanced glucose-stimulated insulin secretion in KO mice on HFD, pancreas sections were stained for both sEH and insulin, and the size of the islets was determined. As previously reported (18), sEH staining is clearly seen throughout the pancreatic islets of WT mice, and absent from the KO mice (Fig. S5). Pancreatic sections from WT, KO, and sEHI-treated mice on chow and HFD were stained for insulin and islet size was determined (Fig. 4 *A*–*C*). On chow diet, KO mice exhibited increased islet size compared with WT. As expected, high fat feeding increased islet size in all groups and led to significantly increased islet size in KO and sEHI-treated mice compared with WT mice (Fig. 4*C*). In

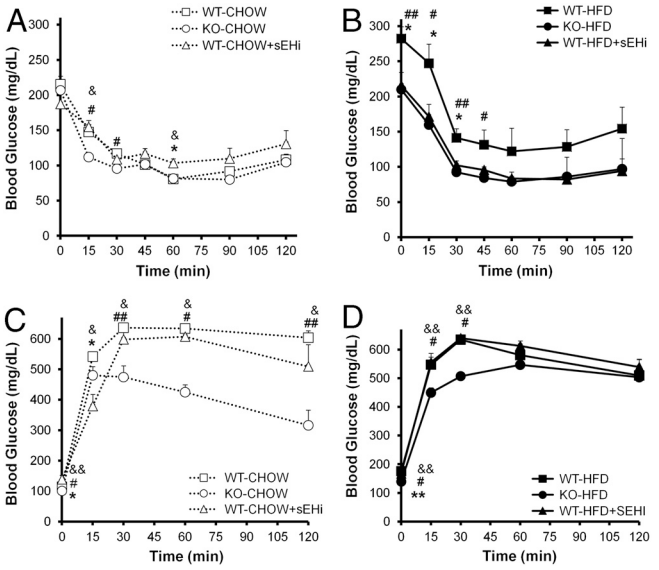

Fig. 3. Reduction of sEH activity prevents diet-induced insulin resistance and sEH-disruption improves glucose tolerance. ITT and GTT were performed on WT, *Ephx2*-null (KO) mice, and sEHI-treated WT male mice ($n = 4$) fed either chow diet (*A*, *C*) or HFD (*B*, *D*) for five months. (*A* and *B*), insulin tolerance test performed by injecting insulin (1 mU/g) i.p. to mice that were fasted four hours prior to ITT. At indicated times, blood samples ($n = 3$) were taken from each animal and glucose was measured using glucometer. (*C* and *D*), glucose tolerance test performed by injecting glucose (2 mg/g of body mass) i.p. to mice that were fasted 16 h prior to GTT. At indicated times, blood samples ($n = 3$) were taken from each animal and glucose was measured using glucometer. Note lower blood glucose levels in both WT with TUPS and KO mice fed HFD at zero time. Values are mean ± SEM (*t*-test) of $n = 4$. *$P \leq 0.05$, **$P \leq 0.01$ WT vs. WT + sEHI; #$P \leq 0.05$, ##$P \leq 0.01$, WT vs. KO; and $P \leq 0.05$, && $P \leq 0.01$ WT + sEHI vs. KO on either diets. All glucose measurements were preformed within the linear range of the Glucometer, and these studies were repeated on younger cohort of mice where the highest blood glucose levels were below 600 mg/dL (Fig. S4 *D* and *F*).

Table 2. Glucose-stimulated insulin secretion during glucose tolerance test

Glucose (mg/dL)	CHOW			HFD		
Time (min)	WT	KO	WT + sEHI	WT	KO	WT + sEHI
0	115 ± 13	101 ± 3*	139 ± 15†	176 ± 9	140 ± 8*	167 ± 3†
15	541 ± 4	480 ± 29	376 ± 39†,‡	547 ± 39	450 ± 17*	553 ± 24†
30	637 ± 14	427 ± 37*	598 ± 33†	634 ± 16	507 ± 13*	639 ± 11†
Insulin (mg/mL)						
Time (min)					KO	
0	0.8 ± 0.05	0.6 ± 0.04	0.8 ± 0.2	0.7 ± 0.06	1.3 ± 0.3*	0.8 ± 0.1
15	5.0 ± 0.05	5.8 ± 0.4	5.2 ± 0.5	6.4 ± 0.6	8.0 ± 1.0	6.4 ± 0.5
30	5.0 ± 0.3	6.5 ± 0.3*	6.6 ± 0.6‡	6.5 ± 0.8	4.8 ± 0.1*	6.3±0.4†

Blood was collected from overnight fasted WT, KO and sEHI-treated WT mice (TUPS, 10 mg/L via drinking water, ad libitum), fed standard chow diet or HFD (test was run after 24 w on diet). The indicated values of glucose and insulin were measured before and after i.p. injection of glucose (2 mg/g of body mass) in mice that were fasted for 16 h. The values are expressed as the means SEM ($n = 4$).

*WT vs. KO

†KO vs. WT + sEHI.

‡WT vs. WT + sEHI

addition, we stained pancreas sections for endothelial cells, using CD31 staining as a marker (Fig. 4*D*). Vascular density, as indicated by the CD31-labeled area in the endocrine pancreas appeared to be enhanced particularly in the KO mice on HFD, and marginally enhanced in sEHI-treated WT mice (Fig. 4*D*). Because VEGF is essential in the regulation of capillary network formation, these data suggest a link among elevated EETs, VEGF, and vascularization and warrants additional investigation.

Increased Insulin Signaling in Liver and Adipose of Mice with Reduced sEH. To investigate the molecular basis for enhanced insulin sensitivity in KO and sEHI-treated mice, we injected mice with insulin or saline (control), and the activation status of components in the insulin signaling pathway was examined in extracts of both liver (Fig. 5) and epididymal adipose (Fig. S6) after HFD. Insulin receptor (IR) immunoprecipitation in the liver and adipose tissue revealed enhanced insulin-induced IR tyrosyl phosphorylation (Y1162/Y1163) in KO and sEHI-treated mice compared with WT mice (Fig. 5 *A* and *B*, Fig. S6 *A* and *B*). Interestingly, the IR was basally hyperphosphorylated in liver extracts of KO mice (Fig. 5 *A* and *B*, at time 0'). Insulin receptor substrate-1 (IRS-1) basal tyrosyl phosphorylation was higher in KO and sEHI-treated mice compared with WT mice (Fig. 5 *C* and *D*). Similarly, IRS-1 tyrosyl phosphorylation (Y608; PI3K binding site) exhibited a comparable pattern but did not reach statistical significance (Fig. 5 *C* and *E*). Moreover, basal and insulin-induced association between p85 subunit of PI3K and IRS-1 was enhanced in KO and sEHI-treated mice compared with WT mice (Fig. 5 *C* and *F*). Consistent with the increased IRS-1 tyrosyl phosphorylation and PI3K binding, insulin stimulated downstream pathway, Akt phosphorylation (Ser473) and MAPK were also enhanced in KO mice and mice treated with TUPS in both tissue homogenates (Fig. 5 *G–J*, Fig. S6 *G–J*).

Discussion

The present study shows that *Ephx2* gene deletion is sufficient to attenuate development of apparent insulin resistance in a murine-model of type 2 diabetes induced by obesity. Loss of sEH activity and the associated stabilization of EETs enhanced insulin-sensitizing actions, increased insulin receptor signaling, and stabilized serum glucose levels. These observations were also supported by pharmacological inhibition of epoxide hydrolase activity. Thus, data from the use of the genetic and pharmacological probe suggest a role for EETs in insulin signaling and glucose homeostasis.

With regard to insulin resistance and metabolic syndrome, reduced sEH activity and the resulting increase in EETs were reported to have a beneficial effect on insulin sensitivity in a diabetes type 1 model (18). It has been reported that cytochrome P450 (CYP 2J,C) expression is decreased and sEH expression is increased in mesenteric arteries of obese Zucker rats (26). On the other hand, streptozotocin-induced diabetic mice have lower sEH expression in liver and kidney, possibly as a result of increase in reactive oxygen species (27). Although this observation suggests a link between bioavailability of EETs and development of metabolic syndrome, the roles of sEH in diabetes are still unclear. The level of expression and the distribution pattern of sEH and CYP450 epoxygenases in any particular tissue may alter the availability of EETs. sEH is ubiquitously expressed including the pancreas, muscle, and adipose. Particularly, sEH is locally expressed in pancreatic islets (18). sEH also regulates adipogenesis and its expression levels are up regulated in response to HFD (17). These observations suggest a direct link between sEH and glucose homeostasis.

In order to clarify the roles of sEH in glucose homeostasis, we used genetically disrupted *Ephx2*-null mice (KO), which have no expression of either the epoxide hydrolase or phosphatase domain. We also used pharmacological inhibition of sEH by

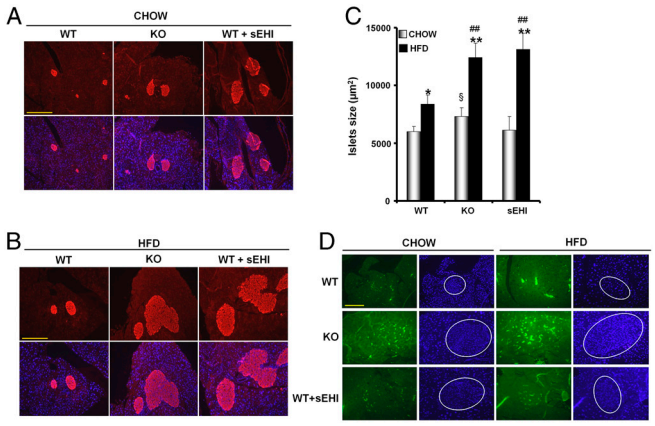

Fig. 4. Islets size and vascularization density in response to Ephx2-gene deletion and inhibition. Representative insulin staining in pancreas sections from WT, KO mice, and sEHI-treated WT at the end of study (6 mo long) either on chow (*A*) or HFD (*B*). Pancreata were stained immunohistochemically for insulin (Red). Bar represents 200 μm. (*C*) Quantitation of islet size as measured by the size of the stained area under the same magnification. * indicates significant difference (*t*-test; $P \leq 0.05$) between diets and # indicates differences (# $P \leq 0.05$; ## $P \leq 0.01$) between WT vs. WT + sEHI or WT vs. KO on HFD; § WT vs. KO on chow diet ($P \leq 0.052$). (*D*) Endothelial cell marker (CD31) staining in pancreatic sections from WT, sEHI-treated WT, and KO mice on chow or HFD. CD31 immunolabeled with specific antibodies (*green*) represents vascular density in the islets (*e.g., inside white boundary*). Vascular density was significantly enhanced in the islets of KO mice and sEHI-treated WT mice on HFD. Nuclei were stained by DAPI (*blue*).

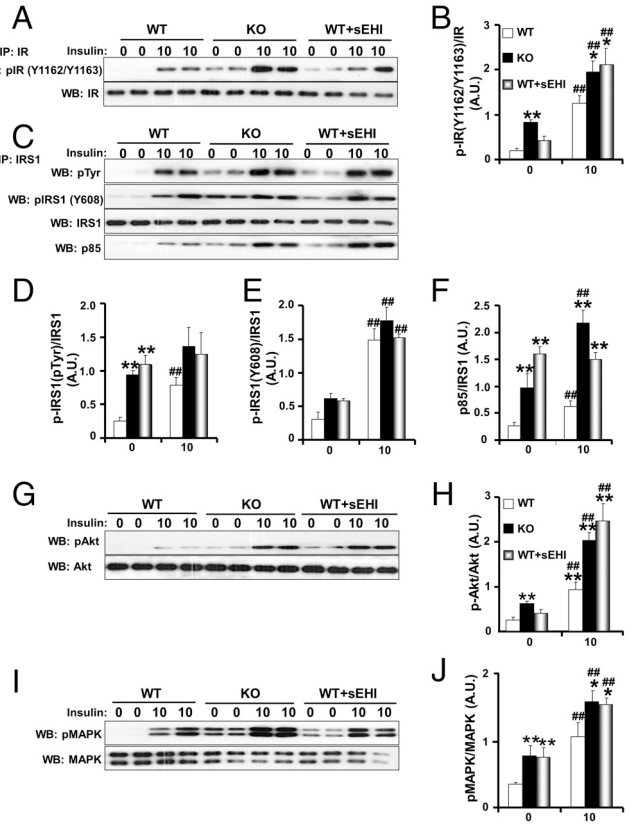

Fig. 5. Enhanced insulin signaling in mice with Ephx2-gene deletion or sEH inhibition. Insulin receptor signaling in liver tissues from male mice on HFD. Mice were fasted overnight then injected i.p. with saline or insulin (10 mU/g) and killed after 10 min. Lysates were immunoprecipitated with IR antibodies, immunoblotted with IR Y^{1162}/Y^{1163} phospho-specific antibodies, and then stripped and reprobed for IR to control for loading. (*C*) IRS1 was immunoprecipitated then immunoblotted with antiphosphotyrosine antibodies, phospho-specific antibodies for Y^{608} and IRS1 antibodies. IRS1 immunoprecipitates were probed using antibodies against the p85 subunit of PI3K. Liver lysates were immunoblotted using anti-Akt Ser473 (*G*), and anti-MAPK (Thr202/Tyr204) (*I*) antibodies. Immunoblots were quantified and bar graphs represent pooled, normalized data (arbitrary units) for KO ($n = 4$) and WT ($n = 4$) mice (*B*, *D–F*, *H*, and *J*). Statistical analysis was performed using one-way ANOVA followed by post hoc *Tukey's* honestly significant difference (HSD) test. * indicates significant difference ($P \leq 0.05$) between WT vs. KO and sEHI-treated mice at 0 or 10 min, while # indicates significant difference within each genotype before and after insulin stimulation.

using a selective sEH inhibitor, TUPS. TUPS is a potent sEHI in vitro, and has no apparent effect on the phosphatase activity of the protein. Thus, we used TUPS to test the hypothesis that the effects observed with *Ephx2*-null mice in the diabetes model were largely due to the absence of the epoxide hydrolase activity. Because this sEHI has high bioavailability and a long half life (21), the high doses used resulted in high blood and tissue levels of TUPS generating a chemical knockout. Previous studies showed that plasma levels of EETs are elevated in the presence of TUPS and in KO mice (22). In spite of the high doses of TUPS, no adverse effects were seen in the pathological analysis of various organs. We provide evidence that both KO and sEHI-treated mice store similar amounts of fat compared with WT mice when provided a hypercaloric diet. As expected from the diet, the high levels of fat dramatically changed organ responses to insulin.

Despite the absence of differences in body weight and/or adiposity in mice fed a HFD, disruption of *Ephx2* led to marked improvements in whole-body glucose homeostasis, indicating that these are primary effects. Basal plasma glucose levels were lower in KO and sEHI-treated mice compared with WT mice. The rate of glucose reduction with insulin injection does not appear different. However, the lower basal levels of plasma glucose can indicate increased insulin production and/or higher insulin signaling. The data from this study suggest that disrupting the *Ephx2* gene or inhibiting its EH activity leads to improved systemic insulin sensitivity and enhanced glucose tolerance. Improved glucose tolerance was seen two but not 5 mo post TUPS treatment. While in the KO mice improved glucose tolerance was consistent throughout the study, suggesting an adaptation to TUPS treatment or some other genetic alteration in the KO mice could be involved.

Glucose homeostasis is maintained by a complex network of signaling events in different cell types and organs including the liver and adipose tissue. Adipocytes can regulate whole-body glucose homeostasis either by the release of insulin-sensitizing adipose-derived hormones (adipokines) or through sequestering excess fatty acids and triglycerides (28, 29) or by decreased responsiveness of insulin receptors and downstream signaling in insulin-responsive tissues (2, 30, 31). Our study revealed that sEH deficiency and inhibition improved insulin signaling in animals on HFD. Biochemical data from liver and adipose tissue of KO and sEHI-treated mice on HFD indicate enhanced insulin signaling in these tissues. Indeed, KO and sEHI-treated mice exhibited increased IR tyrosyl phosphorylation compared with controls. In addition, IRS-1 tyrosyl phosphorylation (32) and PI3K association with IRS-1 were increased in KO and sEHI-treated mice. Moreover, these mice exhibited enhanced insulin-induced Akt and ERK activation. Together, our data suggest that the increased insulin sensitivity of KO and sEHI-treated mice is due, at least in large part, to enhanced insulin signaling in the liver and adipose tissue.

Multiple studies show that sEH inhibition and the resulting increase in EETs exert beneficial vascular and antiinflammatory effects (13, 33). Although diet-induced obesity is defined as a sub inflammatory disease (34–36), we did not observe significant alterations to inflammatory mediators upon sEH deficiency compared with controls. In a different model of insulin resistance due to heme oxygenase 2 gene disruption, the addition of EETs with sEHI caused a marked improvement in all metabolic parameters including inflammatory mediators (37). Another observation from this study is the increase in the size of pancreatic islets and the associated vasculature in both KO and sEHI-treated WT mice. The compensatory response of pancreatic islets to insulin resistance is a recognized feature in obesity and type 2 diabetes. However, the signals and proteins that mediate this important adaptive response are poorly understood (38). Pancreatic islets can respond in vivo to peripheral insulin resistance by increasing their mass through hyperplasia and increased insulin secretion. Furthermore, endothelial cells can affect the ability of pancreatic islets to grow in size when demands for insulin increase (39, 40). A previous study with sEH-null mice in a type 1 diabetes model suggests an increase insulin secretion via reduced apoptotic cell death in islets (18), and the link between CYP2C-derived EETs, VEGF, and endothelial proliferation (41, 42) can also contribute to the large islet size in KO and sEHI-treated mice that were observed in this study.

Previous studies show that disruption of the *Ephx2* gene as well as inhibition of sEH activity by selective inhibitors result in a significant shift of the epoxy-fatty acid to diol ratio (18, 22, 23). Physiological and biochemical insulin signaling data support our conclusion that decreasing sEH and thus increasing plasma levels of EETs provide beneficial effects on glucose regulation possibly through modulating insulin sensitivity.

Materials and Methods

Mouse Studies. Mice with targeted disruption in exon 1 of the *Ephx2* gene (19), were back-crossed onto a C57BL6 (Jackson Laboratories) genetic background an additional ten generations prior to use in this study (20, 43). Mice were placed either on standard chow diet or a HFD (*SI Text*). WT mice were treated with selective sEH inhibitor TUPS 10 mg/L in drinking water (23, 44).

Body Weights, Food Intake, and Organ Weights. Animal body weight along with food intake was monitored weekly. At the end of the feeding period, various fat pads, liver, pancreas, brain, muscle, and kidney were harvested and weighed; one part of the tissues was snap-frozen in liquid nitrogen and stored at −80 °C for further analysis while another part was fixed in 10% formalin or Zinc formalin fixative (*Z*) fix for H and E staining (45).

Metabolic Measurements. Free fatty acid and triglyceride concentrations were measured by an enzymatic colorimetric method (Wako). Serum leptin was assayed by enzyme-linked immunosorbent assay, using mouse leptin standard (Crystal Chem, Inc). Detailed ITT and GTT procedures are described under *SI Text*.

Immunohistochemistry. Pancreas sections (1 μm) were prepared from each sample and stained for insulin as described under *SI Text*. Endothelial cells were stained as previously described (46). Digital images were acquired using a fluorescence microscope (Leica DMI3000B inverted microscope).

Statistical Analyses. Results are presented as means ± standard error of the means (SEM). Comparisons between groups were made by unpaired two-tailed Student's *t* test, Analysis of Variance (ANOVA) or post hoc analysis using Tukey-Kramer honestly significant difference test, as mentioned.

ACKNOWLEDGMENTS. The authors thank Ms. Polly Peirce (Center for Laboratory Animal Science, UC Davis) for breeding and genotyping the mouse colony, Ms. Katie Bell (Center for Comparative Medicine, UC Davis) for tissue processing and sectioning, Dr. Steven Griffen for pathological analysis and Dr. Bart De-Taeye from Northwestern University for critical review of the manuscript. This work was supported by a Junior Faculty Award from the American Diabetes Association (7-06-JF-28) and Research Grant from Juvenile Diabetes Research Foundation (1-2009-337) to (F.G.H). National Institute of Environmental Health Sciences, R01 ES002710 (B.D.H); National Heart, Lung, and Blood Institute R01 HL059699 (J.D.I); National Institute of Environmental Health Sciences Superfund Basic Research Program, P42 ES004699 (B.D.H) and UC Tobacco-Related Disease Research Program New Investigator Award 16KT-0037 (A.L). B.D. Hammock is a George and Judy Marcus Senior Fellow of the American Asthma Foundation.

1. Smyth S, Heron A (2006) Diabetes and obesity: the twin epidemics. *Nat Med* 12:75–80.
2. Biddinger SB, Kahn CR (2006) From mice to men: insights into the insulin resistance syndromes. *Annu Rev Physiol* 68:123–158.
3. Lizcano JM, Alessi DR (2002) The insulin signalling pathway. *Curr Biol* 12:R236–238.
4. Luo J, Cantley LC (2005) The negative regulation of phosphoinositide 3-kinase signaling by p85 and it's implication in cancer. *Cell Cycle* 4:1309–1312.
5. Avruch J (1998) Insulin signal transduction through protein kinase cascades. *Mol Cell Biochem* 182:31–48.
6. Shulman GI (2000) Cellular mechanisms of insulin resistance. *J Clin Invest* 106:171–176.
7. Kobayashi K (2005) Adipokines: therapeutic targets for metabolic syndrome. *Current Drug Targets* 6:525–529.
8. Zhang CY, et al. (2001) Uncoupling protein-2 negatively regulates insulin secretion and is a major link between obesity, beta cell dysfunction, and type 2 diabetes. *Cell* 105:745–755.
9. Taniguchi CM, Emanuelli B, Kahn CR (2006) Critical nodes in signalling pathways: insights into insulin action. *Nature Reviews* 7:85–96.
10. Oliw EH (1994) Oxygenation of polyunsaturated fatty acids by cytochrome P450 monooxygenases. *Prog Lipid Res* 33:329–354.
11. Larsen BT, Campbell WB, Gutterman DD (2007) Beyond vasodilatation: non-vasomotor roles of epoxyeicosatrienoic acids in the cardiovascular system. *Trends Pharmacol Sci* 28:32–38.
12. Inceoglu B, et al. (2011) Analgesia mediated by soluble epoxide hydrolase inhibitors is dependent on cAMP. *Proc Natl Acad Sci USA* 108:5093–5097.
13. Schmelzer KR, et al. (2005) Soluble epoxide hydrolase is a therapeutic target for acute inflammation. *Proc Natl Acad Sci USA* 102:9772–9777.
14. Newman JW, Morisseau C, Hammock BD (2005) Epoxide hydrolases: their roles and interactions with lipid metabolism. *Prog Lipid Res* 44:1–51.
15. Yu Z, et al. (2000) Soluble epoxide hydrolase regulates hydrolysis of vasoactive epoxyeicosatrienoic acids. *Circ Res* 87:992–998.
16. Ohtoshi K, et al. (2005) Association of soluble epoxide hydrolase gene polymorphism with insulin resistance in type 2 diabetic patients. *Biochem Biophys Res Commun* 331:347–350.
17. De Taeye BM, et al. (2010) Expression and regulation of soluble epoxide hydrolase in adipose tissue. *Obesity,* (Silver Spring, MD), 18, pp 489–498.
18. Luo P, et al. (2010) Inhibition or deletion of soluble epoxide hydrolase prevents hyperglycemia, promotes insulin secretion, and reduces islet apoptosis. *J Pharmacol Exp Ther* 334:430–438.
19. Sinal CJ, et al. (2000) Targeted disruption of soluble epoxide hydrolase reveals a role in blood pressure regulation. *J Biol Chem* 275:40504–40510.
20. Luria A, et al. (2007) Compensatory mechanism for homeostatic blood pressure regulation in Ephx2 gene-disrupted mice. *J Biol Chem* 282:2891–2898.
21. Liu JY, et al. (2009) Pharmacokinetic optimization of four soluble epoxide hydrolase inhibitors for use in a murine model of inflammation. *Br J Pharmacol* 156:284–296.
22. Enayetallah AE, et al. (2008) Opposite regulation of cholesterol levels by the phosphatase and hydrolase domains of soluble epoxide hydrolase. *J Biol Chem* 283:36592–36598.
23. Jones PD, Tsai HJ, Do ZN, Morisseau C, Hammock BD (2006) Synthesis and SAR of conformationally restricted inhibitors of soluble epoxide hydrolase. *Bioorg Med Chem Lett* 16:5212–5216.
24. Hwang SH, Tsai HJ, Liu JY, Morisseau C, Hammock BD (2007) Orally bioavailable potent soluble epoxide hydrolase inhibitors. *J Med Chem* 50:3825–3840.
25. Kadowaki T, Yamauchi T (2005) Adiponectin and adiponectin receptors. *Endocrine Rev* 26:439–451.
26. Zhao X, et al. (2005) Decreased epoxygenase and increased epoxide hydrolase expression in the mesenteric artery of obese Zucker rats. *Am J Physiol-Reg I* 288:R188–196.
27. Oguro A, Fujita N, Imaoka S (2009) Regulation of soluble epoxide hydrolase (sEH) in mice with diabetes: high glucose suppresses sEH expression. *Drug metab pharmacok* 24:438–445.
28. Tontonoz P, Spiegelman BM (2008) Fat and beyond: the diverse biology of PPARgamma. *Annu Rev Biochem* 77:289–312.
29. Rader DJ (2007) Effect of insulin resistance, dyslipidemia, and intra-abdominal adiposity on the development of cardiovascular disease and diabetes mellitus. *Am J Med* 120(3 Suppl 1):S12–18.
30. Uysal KT, Wiesbrock SM, Marino MW, Hotamisligil GS (1997) Protection from obesity-induced insulin resistance in mice lacking TNF-alpha function. *Nature* 389:610–614.
31. Farese RV (2001) Insulin-sensitive phospholipid signaling systems and glucose transport. Update II. *Exp Biol Med (Maywood)* 226:283–295.
32. Schmitz-Peiffer C, Whitehead JP (2003) IRS-1 regulation in health and disease. *International Union of Biochemistry and Molecular Biology Life* 55:367–374.
33. Yang S, et al. (2007) Cytochrome P-450 epoxygenases protect endothelial cells from apoptosis induced by tumor necrosis factor-alpha via MAPK and PI3K/Akt signaling pathways. *Am J Physiol Heart Circ Physiol* 293:H142–151.
34. Xu H, et al. (2003) Chronic inflammation in fat plays a crucial role in the development of obesity-related insulin resistance. *J Clin Invest* 112:1821–1830.
35. Lumeng CN, Deyoung SM, Bodzin JL, Saltiel AR (2007) Increased inflammatory properties of adipose tissue macrophages recruited during diet-induced obesity. *Diabetes* 56:16–23.
36. Kubota N, et al. (1999) PPAR gamma mediates high-fat diet-induced adipocyte hypertrophy and insulin resistance. *Mol Cell* 4:597–609.
37. Sodhi K, et al. (2009) Epoxyeicosatrienoic acid agonist rescues the metabolic syndrome phenotype of HO-2-null mice. *J Pharmacol Exp Ther* 331:906–916.
38. Flier SN, Kulkarni RN, Kahn CR (2001) Evidence for a circulating islet cell growth factor in insulin-resistant states. *Proc Natl Acad Sci USA* 98:7475–7480.
39. Lammert E, et al. (2003) Role of VEGF-A in vascularization of pancreatic islets. *Curr Biol* 13:1070–1074.
40. Nikolova G, et al. (2006) The vascular basement membrane: a niche for insulin gene expression and Beta cell proliferation. *Dev Cell* 10:397–405.
41. Potente M, Michaelis UR, Fisslthaler B, Busse R, Fleming I (2002) Cytochrome P450 2C9-induced endothelial cell proliferation involves induction of mitogen-activated protein (MAP) kinase phosphatase-1, inhibition of the c-Jun N-terminal kinase, and up-regulation of cyclin D1. *J Biol Chem* 277:15671–15676.
42. Webler AC, et al. (2008) Epoxyeicosatrienoic acids are part of the VEGF-activated signaling cascade leading to angiogenesis. *Am J Physiol* 295:C1292–1301.
43. Luria A, et al. (2009) Alteration in plasma testosterone levels in male mice lacking soluble epoxide hydrolase. *Am J Physiol-Endoc M* 297:E375–383.
44. Chiamvimonvat N, Ho CM, Tsai HJ, Hammock BD (2007) The soluble epoxide hydrolase as a pharmaceutical target for hypertension. *J Cardiovasc Pharmacol* 50:225–237.
45. Kushner JA, et al. (2004) Islet-sparing effects of protein tyrosine phosphatase-1b deficiency delays onset of diabetes in IRS2 knockout mice. *Diabetes* 53:61–66.
46. Kostromina E, et al. (2010) Glucose intolerance and impaired insulin secretion in pancreas-specific signal transducer and activator of transcription-3 knockout mice are associated with microvascular alterations in the pancreas. *Endocrinology* 151:2050–2059.